

Power System Voltage Stability Analysis

Chemikala Madhava Reddy

A Thesis Submitted to
Indian Institute of Technology Hyderabad
In Partial Fulfillment of the Requirements for
The Degree of Master of Technology



Department of Electrical Engineering

June 2011

Declaration

I declare that this written submission represents my ideas in my own words, and where ideas or words of others have been included, I have adequately cited and referenced the original sources. I also declare that I have adhered to all principles of academic honesty and integrity and have not misrepresented or fabricated or falsified any idea/data/fact/source in my submission. I understand that any violation of the above will be cause for disciplinary action by the Institute and can also evoke penal action from the sources that have thus not been properly cited, or from whom proper permission has not been taken when needed.

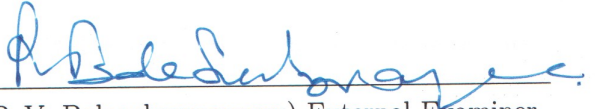
C. Madhava Reddy
(Signature)

Chemikala Madhava Reddy
Student Name

EE09G003
Roll No

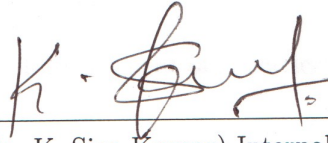
Approval Sheet

This thesis titled "Power System Voltage Stability Analysis" by Mr. Chemikala Madhava Reddy is approved for the degree of Master of Technology.



(Dr. P. V. Balasubramanyam) External Examiner

CPRI



(Dr. K. Siva Kumar) Internal Examiner

Dept. of Elec Engg

IITH



(Dr. Vaskar Sarkar) Research Supervisor

Dept. of Elec Engg

IITH



(Dr. R. Prasanth Kumar) Chairman

Dept. of Mech Engg

IITH

Acknowledgements

First and foremost, my utmost gratitude to Dr. Vaskar Sarkar, my thesis supervisor whose sincerity and encouragement I will never forget. He has been inspiration to me and my colleagues without which this work is not possible at all. He motivated me very much and corrected many times.

I am very grateful to our Director Prof. U. B. Desai for providing us with an environment to complete our thesis work successfully.

I am deeply indebted to our Head of the Department Prof. R. D. Koilpillai, who inspired us think in inter disciplinary concepts.

I would like to thank all the faculty members of department of Electrical engineering, IIT Hyderabad for their constant encouragement.

I am thankful to the faculty members of department of Electrical engineering, IIT Madras for inspiring me at the beginning of my master's program.

I thankful to Ordnance Factory, Medak for the beautiful campus which made my stay a cool one.

I am ever grateful to my institute, IIT Hyderabad for providing the necessary infrastructure and financial support. I thank the academic and non-academic staff of IIT Hyderabad for their prompt and generous help. I would also like to thank the computer lab, IIT Hyderabad for providing excellent computation facilities.

I would like to thank all my M.Tech friends. Finally I thank my parents for allowing me to continue my studies.

Chemikala Madhava Reddy

To
my Parents and Teachers

Abstract

Power system is facing new challenges as the present system is subjected to severely stressed conditions. Voltage instability is a quite frequent phenomenon under such a situation rendering degradation of power system performance. In order to avoid system blackouts, power system is to be analyzed in view of voltage stability for a wide range of system conditions.

In voltage stability analysis, the main objective is to identify the system maximum loadability limit and causes of voltage instability. Static voltage stability analysis with some approximations gives this information. Voltage stability problem is related to load dynamics and therefore different load characteristics are to be considered in the voltage stability analysis.

In this work, the first objective is to find out the maximum loadability limit by using various methods. Initially, the maximum loadability limit is calculated by using P-V and Q-V curve methods. However these two methods are quite time consuming because of successive power flow studies. To reduce computational time, continuation power flow method is used and it also provides information about voltage sensitive buses. From these methods, buses with least stability margin are identified as critical buses.

The second objective of this work is to find out the causes of voltage instability. Modal analysis is performed and critical buses, critical lines are identified using participation factors. For critical buses, Q-V curves are generated and their reactive power margins are calculated to crosscheck the modal analysis result. Voltage stability indices which provides an accurate information about line and bus stability conditions are studied for various loading scenarios. The different voltage stability indices are calculated and compared for IEEE standard 14 bus system.

Contents

Abstract	i
List of Figures	v
List of Tables	vi
Nomenclature	x
1 Introduction	1
1.1 Background	1
1.2 Voltage Stability Problem	2
1.3 Literature Review	3
1.4 Outline of the Thesis	6
2 Elements of Voltage Stability	7
2.1 Introduction	7
2.2 Classification of Power System Stability	7
2.3 Definitions of Voltage Stability	8
2.3.1 Definitions according to CIGRE	8
2.3.2 Definitions according to Hill and Hiskens	9
2.3.3 Definitions according to IEEE	9
2.4 Causes of Voltage Instability	10
2.5 Loading Margin	11
2.6 Bifurcation Analysis	12
2.7 Examples of Voltage Instability	13

3	Load Modeling and Countermeasures for Voltage Collapse	17
3.1	Introduction to Load Modeling	17
3.1.1	Static Load Modeling	17
3.1.2	Dynamic Load Modeling	19
3.2	Countermeasures for Voltage Collapse	20
4	Methods of Voltage Stability Analysis	23
4.1	Introduction	23
4.2	Real Power Margin Computation Using The P-V curve	24
4.3	Reactive Power Margin Computation Using The Q-V curve	25
4.4	Disadvantages of P-V curves and Q-V curves	27
4.5	Minimum Singular Value Method	27
4.6	Continuation Power Flow Method	28
4.6.1	Critical point identification	30
4.7	Modal Analysis	30
4.7.1	Identification of critical buses and branches	33
4.8	Voltage Stability Indices	33
4.8.1	Fast Voltage Stability Index (FVSI)	34
4.8.2	Line stability index L_{mn}	36
4.8.3	Voltage reactive power index VQI	36
4.8.4	Voltage stability index L	37
4.9	Simulation Results and Discussions	37
4.9.1	Introduction	37
4.9.2	Results for IEEE standard 6-Bus system	38
4.9.3	Results for IEEE Standard 14-bus System	43
5	Conclusions and Future Scope of Research	51
5.1	Conclusions	51
5.2	Future Scope of Research	52
	Bibliography	53

List of Figures

2.1	Classification of power system stability [1].	8
2.2	Acting time scale of power system devices [7].	12
2.3	Loading margin of a simple system.	13
2.4	Single line diagram of a two bus system.	14
2.5	Variation of voltage with real power for different power factors.	15
2.6	Loss of equilibrium with gradual increase in load.	15
2.7	Reduced voltage stability margin following a disturbance.	16
4.1	Typical P-V curve.	25
4.2	Typical Q-V curve.	26
4.3	2-bus power system model.	34
4.4	The P-V curves of load buses for constant power load of IEEE 6-bus power system.	38
4.5	The P-V curves of load buses for constant current load of IEEE 6-bus power system.	39
4.6	The Q-V curves of load buses of IEEE 6-bus power system.	40
4.7	Critical loading factor using Continuation power flow method.	41
4.8	Path of minimum eigenvalue with increase of loading.	41
4.9	Bus Participation factors for most critical modes for the IEEE 6-bus system.	42
4.10	Branch Participation factors for most critical modes for the IEEE 6-bus system.	42
4.11	The P-V curves of IEEE 14 bus system for constant load model.	43
4.12	Real power margin for constant power load model of IEEE 14-bus system.	43

4.13	The P-V curves for constant current load model of IEEE 14-bus system. . .	44
4.14	Real power margin for constant current load model of IEEE 14-bus system.	44
4.15	Reduced Real power margin of Bus 14 following the outage of line 9-14. . .	45
4.16	The Q-V curves for constant power load model of IEEE 14-bus system. . .	46
4.17	Reactive power margin for constant power load model of IEEE 14-bus system.	47
4.18	Path of minimum eigenvalue with increase of load for IEEE 14-bus system.	47
4.19	Bus participation factors for IEEE 14-bus system.	48
4.20	Branch participation factors for IEEE 14-bus system.	48
4.21	The variation of voltage stability indices FVSI, LMN and VQI for critical branch with loading factor λ	49
4.22	The variation of line stability index L, voltage of bus 14 with loading factor λ	49
4.23	The variation of voltage stability indices FVSI, LMN and VQI with loading factor λ for multiple load increase scenario.	50
4.24	The variation of line stability index L, voltage of bus 14 with loading factor λ for multiple load increase scenario.	50

List of Tables

3.1	Typical values for exponents of load model [3]	18
4.1	Real power margin of load buses for constant power load model of IEEE 6-bus system	38
4.2	Real power margin of load buses for constant current load model of IEEE 6-bus system	39
4.3	Reactive power margin of load buses of IEEE 6-bus system	40
4.4	Comparison of Real power margin of Critical buses 14, 10 and 9 using P-V curves and CPF method	45

Nomenclature

List of Symbols

P	Real power
Q	Reactive power
J	Jacobian matrix of the power system
J_R	Reduced system Jacobian matrix
ΔV	Change in the voltage value
ΔQ	Change in the reactive power
P_0	Steady state value of the load real power
Q_0	Steady state value of the load reactive power
P_m	maximum real power drawn by the load
Q_m	maximum reactive power drawn by the load
V	Voltage
I	Current
R	Resistance
X	Reactance
S	Apparent power

Z_p	Component of constant impedance load in load real power
I_p	Component of constant current load in load real power
P_p	Component of constant power load in load real power
Z_q	Component of constant impedance load in load reactive power
I_q	Component of constant current load in load reactive power
P_q	Component of constant power load in load reactive power
T_p	Recovery time constant of dynamic load
α_s	Exponent of static load real power
α_i	Exponent of instantaneous real power
P_s	Steady state real power load
P_i	Instantaneous real power load
P_d	Final consumed load real power
K_L	Load increment factor
ΔP_i	Real power mismatch at bus i^{th} bus
ΔQ_i	Reactive power vector mismatch at i^{th} bus
P_{Gi}	Real power generation at i^{th} bus
P_{Li}	Real power consumption at i^{th} bus
P_{Inji}	Real power injection at i^{th} bus
T	Tangent vector
e_k	Approximately row dimensioned vector with ± 1
ΔQ_{mi}	Modal reactive power variation corresponding to i^{th} mode.

ΔV_{mi}	Modal voltage variation corresponding to i^{th} mode.
K_i	Normalization factor
P_{ki}	Bus participation factor of k^{th} bus for critical mode i
P_{lji}	Branch participation factor of branch l-j for critical mode i
ΔQ_{lji}	Linearized reactive power loss across branch l-j
\bar{I}^G	Generator current vector
\bar{I}^L	Load current vector
\bar{V}^G	Generator voltage vector
\bar{V}^L	Load voltage vector
λ	Loading factor of a bus
λ_{cr}	Loading factor corresponding to critical load
δ	Angle of a bus
α	exponent of voltage dependent real power load
β	exponent of voltage dependent reactive power load
σ	Scalar designating the step size
η	Left eigenvector of reduced Jacobian matrix J_R
ξ	Right eigenvector of reduced Jacobian matrix J_R
Λ	Diagonal eigenvalue matrix of J_R
ϕ	power factor angle of the load

List of Acronyms

LTC	Load Tap Changer
-----	------------------

DVR	Distribution Voltage Regulator
CPF	Continuation Power Flow method
FVSI	Fast Voltage Stability Index
LMN	Line Voltage Stability Index
VQI_{Line}	Voltage Reactive Power Index
SVC	Static VAR Compensator
OEL	Over Excitation Limiter
SCL	Stator Current Limiter
SNB	Saddle-Node Bifurcation
ZIP	Polynomial Load Model

Chapter 1

Introduction

1.1 Background

Modern power systems are operating under very stressed conditions and this is making the system to operate closer to their operating limits. Operation of power system is becoming difficult owing to the following reasons:

- Increased competition in power sector.
- Social and environmental burdens; resulting to limited expansion of transmission network.
- Lack of initiatives to replace the old voltage and power flow control mechanisms.
- Imbalance in load-generation growth.

All these factors are causing power system stability problems. A power system operating under stressed conditions shows a different behavior from that of a non-stressed system. As the system is operating close to the stability limit, a relatively small disturbance may causes the system to become unstable. As the power system is normally a interconnected system, it's operation and stability will be severely affected.

1.2 Voltage Stability Problem

Voltage stability problem is significant since it affects the power system security and reliability. Voltage stability [1] is related to the “ability of a power system to maintain acceptable voltages at all buses under normal conditions and after being subjected to a disturbance”. Definitions proposed by various authors related to voltage stability are mentioned in Chapter 2. Voltage instability is an aperiodic, dynamic phenomenon. As most of the loads are voltage dependent and during disturbances, voltages decrease at a load bus will cause a decrease in the power consumption. However loads tend to restore their initial power consumption with the help of Distribution Voltage Regulators, Load Tap Changers (LTC) and thermostats. These control devices try to adjust the load side voltage to their reference voltage. The increase in voltage will be accompanied by an increase in the power demand which will further weaken the power system stability. Under these conditions voltages undergo a continuous decrease, which is small at starting and leads to voltage collapse.

When a single machine is connected to a load bus then there will be pure voltage instability. When a single machine is connected to infinite bus then there will be pure angle instability. When synchronous machines, infinite bus and loads are connected then there will be both angle and voltage instability but their influence on one another can be separated [2]. The dynamics involved in voltage instability are restricted to load buses with LTC, restorative loads etc.,. These load voltage control devices are operated for few minutes to several minutes. So, generator dynamics can be substituted by appropriate equilibrium conditions. Under stressed conditions, coupling between voltage and active power is not weak [3]. So, insufficient active power in the system also leads to voltage instability problems.

The following are the main contributing factors [3] to voltage instability problem.

- Increased stress on power system.
- Insufficient reactive power resources.

- Load restoring devices in response to load bus voltages.
- Unexpected and or unwanted relay operation following a drop in voltage magnitude
- Line or generator outages.
- Increased consumption in heavy load centers.

Even though voltage instability phenomenon is dynamic in nature, both static and dynamic analysis methods [4] are used. To operate the system safely, system is to be analyzed for various operating conditions and contingencies. In most cases, the system dynamics affecting voltage stability are usually quite slow and much of the problem can be analyzed using static analysis that gives information about the maximum loadability limit [3] and factors contributing to instability problem. Static approach involves computation of only algebraic equations and it is faster than dynamic approach. Static analysis takes less computational time compared to dynamic analysis and conventional power flow is used in the static analysis. A number of static voltage stability analysis methods [5] are proposed in the literature for analyzing the problem.

1.3 Literature Review

The fundamental concepts of power system modeling and operation are discussed in [6]. The stability problems involved in power system operation are well presented in [1]. Types of voltage stability and factors affecting it are well explained in [3] [7].

Voltage stability and Rotor angle stability problems occurs in same time-frame and thus both are interlinked. Although both are interlinked, in may cases, one form of instability predominates. The relation between rotor angle stability and voltage stability is explained in [2] [7].

There are various methods [8] used for static voltage stability analysis. The most applied method for indicating voltage stability limit is by calculating system load margin.

The two most widely used indicators are real power (P) margin, and the reactive power (Q) margin.

In P-V curve [3], real power at a bus or area is gradually increased by keeping power factor constant. Successive power flow studies are done until the bifurcation point or nose point is reached. The points above the nose point corresponds to stable operating condition. We can use continuation power flow method to find the solutions below the operating point, which is not necessary. In this curve the nose point represents the maximum real power loading point. Real power margin is the distance between present operating point to critical operating point. Since power flow calculations are involved in generating P-V curves, it takes lot of time for large networks. P-V curves gives only proximity to critical point but no information about causes of voltage stability problem.

Reactive power margin is computed by using Q-V curve [6]. For scheduled bus voltages, the reactive power to be injected or drawn is calculated from successive power flow. The reactive power margin is the difference of reactive power at present operating point and minimum reactive power. The calculated reactive power margin is helpful to find the size of shunt compensator. Similarly to the P-V curve, Q-V curve also provides no information about key contributing factors to voltage stability problem and computational time is also high.

Minimum singular value method proposed by Thomas and Lof [9] is used to calculate the voltage stability margin by observing how close is the Jacobian matrix to become singular. In the analysis, load value is increased in steps and power flow Jacobian matrix J is calculated. Whenever the smallest singular value of J reaches zero, it is inferred that loadability limit is reached. This method however, cannot find the specific causes for voltage instability. Although it gives relative proximity to voltage stability limit but is not a absolute or linear measurement. This is due to the non-linear behavior shown by the system after stable operating point up to the bifurcation point.

Continuation power flow (CPF) method proposed by Venkataramana Ajjarapu [10]

is used for finding the continuous power flow solutions starting from base load condition to steady state voltage stability limit. The main difference between CPF and conventional power flow method can be observed as the operating point approaches critical point. In conventional power flow as the operating point comes close to critical point, power flow will not converge. In CPF method, divergence problem doesn't arise and it uses predictor-corrector [11] process to find the next operating point. As the critical point is approached, loading factor λ reaches maximum and starts decreasing. The tangent component corresponding to λ is zero at critical point and becomes negative after that. From the tangent vector, information about weak buses can be obtained.

Using Modal analysis [12] proposed by Gao, Morrison and Kundur in 1992, the reactive power margin and voltage instability contributing factors are calculated. Modal analysis depends on power flow Jacobian matrix. Real power is kept constant and reduced Jacobian matrix J_R of the system is calculated. The matrix J_R represents the linearized relationship between the incremental changes in bus voltage (ΔV) and the bus reactive power injection (ΔQ). If the minimum eigenvalue of J_R is greater than zero, the system is voltage stable. Using the left and right eigenvectors corresponding to critical mode, bus participation factors can be calculated. Branch participation factors are calculated from linearized reactive power loss. Buses and Branches with large participation factors are identified as critical buses.

Voltage stability indices are helpful in determining the proximity of a given operating point to voltage collapse point. These indices are simple, easy to implement and computationally inexpensive. Voltage stability indices can be used for both on-line or off-line studies. In literature, several indices are proposed. Voltage stability indices are derived from power flow equations. Fast Voltage Stability Index (FVSI) proposed by I.Musirin et al. [13], line stability index L_{mn} proposed by M.Moghavemani et al. [14], Voltage Reactive Power Index (VQI_{Line}) proposed by M.W.Mustafa et al, [15] and L index proposed by P.Kessel et al. [16] are calculated for IEEE standard 14 bus system for various loading scenarios. If the index value approaches one then it is inferred that voltage collapse point is reached. These indices gives the information regarding critical

buses and branches.

1.4 Outline of the Thesis

Chapter 1 presents a brief introduction to voltage stability problem along with a literature survey.

Chapter 2 gives general background of the voltage stability phenomena and its types. Voltage instability phenomena is explained with few examples.

Chapter 3 presents load modeling for voltage stability analysis and counter measures for voltage instability.

chapter 4 presents various static voltage analysis methods along with simulation results.

Chapter 5 concludes the work and shows the future scope of work.

Chapter 2

Elements of Voltage Stability

2.1 Introduction

Voltage stability is a problem in power systems which are heavily loaded, faulted or have shortage of reactive power. The nature of voltage stability can be analyzed by examining the production, transmission and consumption of reactive power. The problem of voltage stability concerns the whole power system, although it usually has a large involvement in one critical area of the power system. In this chapter, voltage stability, voltage instability and voltage collapse are defined and then voltage stability types are mentioned. Concepts of loading margin and bifurcation analysis are briefly explained. The importance of load modeling and various load models are listed out. Voltage stability is described using a simple example.

2.2 Classification of Power System Stability

A definition of power system stability as given in [1] is:

Power system stability is the ability of an electric power system, for a given initial operating condition, to regain a state of operating equilibrium after being subjected to a physical disturbance, with most system variables bounded so that practically the entire system remains intact.

Classification of power system stability [1] is shown in Figure 2.1.

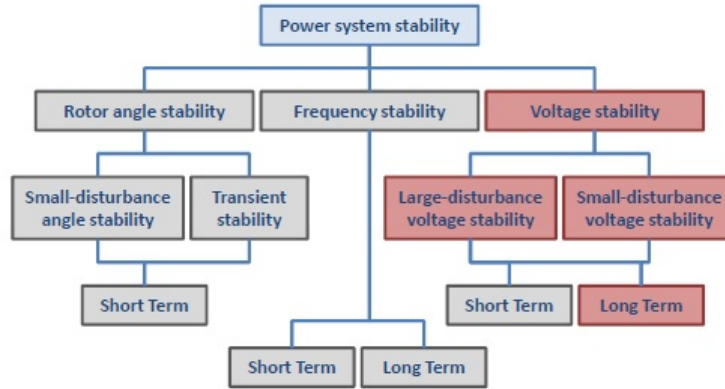


Figure 2.1: Classification of power system stability [1].

2.3 Definitions of Voltage Stability

In literature several definitions of voltage stability are found which are based on time frames, system states, size of disturbance etc. During voltage instability, a broad spectrum of phenomena will occur.

2.3.1 Definitions according to CIGRE

CIGRE [1] defines voltage stability in a general way similar to other dynamic stability problems. According to CIGRE,

- A power system at a given operating state is *small-disturbance voltage stable* if, following any small disturbance, voltages near loads are identical or close to the pre-disturbance values.
- A power system at a given operating state and subject to a given disturbance is *voltage stable* if voltages near loads approach post-disturbance equilibrium values. The disturbed state is within the region of attraction of the stable post-disturbance equilibrium.
- A power system undergoes *voltage collapse* if the post-disturbance equilibrium voltages are below acceptable limits.

2.3.2 Definitions according to Hill and Hiskens

Hill and Hiskens proposes definitions which is divided into a static and dynamic part. For the system to be stable, the static part of the following must be true.

- The voltages must be viable i.e. they must lie within an acceptable band.
- The power system must be in a voltage regular operating point.

A regular operating point implies that if reactive power is injected into the system or a voltage source increases its voltage, a voltage increase is expected in the network. For the dynamic behavior of the phenomena the following are the concepts:

- *Small disturbance voltage stability*: A power system at a given operating state is small disturbance stable if following any small disturbance, its voltages are identical to or close to their pre-disturbance equilibrium values.
- *Large disturbance voltage stability*: A power system at a given operating state and subject to a given large disturbance is large disturbance voltage stable if the voltages approach post-disturbance equilibrium values.
- *Voltage collapse*: A power system at a given operating state and subject to a given large disturbance undergoes voltage collapse if it is voltage unstable or the post-disturbance equilibrium values are nonviable.

2.3.3 Definitions according to IEEE

According to IEEE [1], the following formal definitions of terms related to voltage stability are given:

- *Voltage Stability* is the ability of a system to maintain voltage so that when load admittance is increased, load power will increase, and so that both power and voltage are controllable.
- *Voltage Collapse* is the process by which voltage instability leads to loss of voltage in a significant part of the system.

- *Voltage Security* is the ability of a system, not only to operate stably, but also to remain stable (as far as the maintenance of system voltage is concerned) following any reasonably credible contingency or adverse system change.

In a more general way, voltage stability according to Van Cutsem [3],

Voltage instability stems from the attempt of load dynamics to restore power consumption beyond the capability of the combined transmission and generation system.

2.4 Causes of Voltage Instability

There are three main causes of voltage instability:

1. Load dynamics: Loads are the driving force of voltage instability. Load dynamics are due to the following devices.
 - Load tap changing (LTC) transformer role [16] is to keep the load side voltage in a defined band near the rated voltage by changing the ratio of transformer. As most of the loads are voltage dependent, a disturbance causing a voltage decrease at a load bus will cause a decrease in the power consumption. This tends to favor stability. However, the LTC will then begin to restore the voltage by changing the ratio step by step with a predefined timing. The increase in voltage will be accompanied by an increase in the power demand which will further weaken the power system stability.
 - Thermostat will control the electrical heating. The thermostat acts by regularly switching the heating resistance on and off. In the case of a voltage decrease, the power consumption, hence the heating power, will be reduced. Therefore, the thermostat will tend to supply the load during a longer time interval. The aggregated response of a huge group of this kind of loads is seen as a restoration of the power, comparable to the one of the LTC.

- Induction motors have dynamic characteristics with short time constants. Restoration process occurs following voltage reduction because the motor must continue to supply a mechanical load with a torque more or less constant.
2. Transmission system: Each transmission element, line or transformer, has a limited transfer capability. It is dependent on several factors:
 - The impedance of the transmission element.
 - The power factor of the load.
 - The presence of voltage controlled sources (generators or Static Var Compensator-SVC) at one or both extremities of the element and the voltage set point of these sources.
 - The presence of reactive compensation devices (mechanically switched capacitors or reactors).
 3. Generation system: When the power system flows increase, the transmission system consumes more reactive power. The generators must increase their reactive power output. Operating point of generator can be found from it's capability curve. But due to over-excitation limiter (OEL) and stator current limiter (SCL), voltage can't be controlled after these limiters are activated.

As described above, the three sources are strongly linked one to another. In a real voltage collapse case, the complete instability mechanism generally involves all three aspects, and often other instability phenomena too. The following Figure 2.2 shows the act of power system devices in voltage collapse in different time-frames.

2.5 Loading Margin

The proximity to voltage collapse can be determined by means of several indices. A very common index is the loading margin which is calculated based on loadability limit. For a particular operating condition, loadability limit [3] is defined as the maximum loading point after which there will be no operating point. Power flow equation will

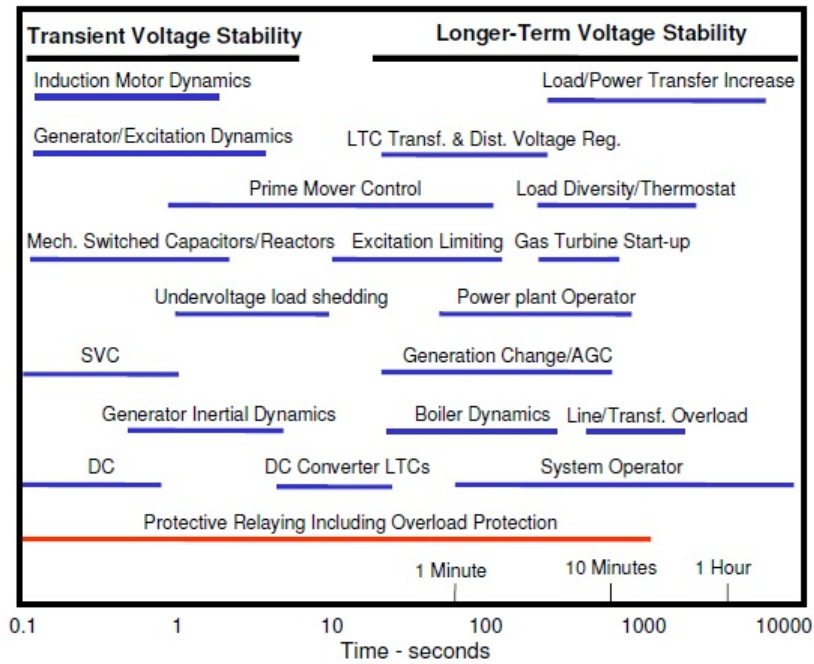


Figure 2.2: Acting time scale of power system devices [7].

not have solution beyond loadability limit. P-V and Q-V curves are the most used to determine the loading margin of a power system at an individual load bus. Real power loading margin is shown in Figure 2.3.

In Figure 2.3, P_0 is the base case load real power and P_m is the maximum load real power. Loading margin is calculated as the difference of P_m and P_0 .

2.6 Bifurcation Analysis

Voltage stability is a non-linear phenomenon and bifurcation theory is one of the non-linear techniques used for the voltage stability analysis. Bifurcation describes qualitative changes such as loss of stability. Bifurcation theory assumes that power system parameters vary slowly and predicts how a power system becomes unstable. Usually load demand is the parameter that is varied and there is a possibility to achieve either Saddle Node Bifurcation (SNB) or Hopf bifurcation [11].

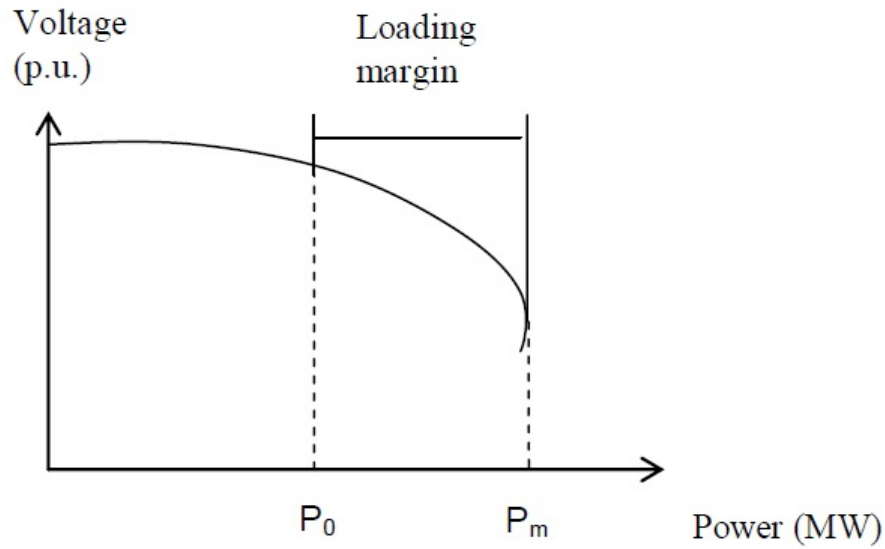


Figure 2.3: Loading margin of a simple system.

Static loadability limit is associated with SNB and limit-induced bifurcations. These bifurcations consist loss of system equilibrium, which is typically correlated with the lack of power flow solutions. In SNB, at saddle node point the stable and unstable equilibrium points coalesce and disappear. At SNB, system Jacobian matrix is singular, thus one of eigenvalues must be zero. After the loss of operating equilibrium, the system voltages fall dynamically. In case of Hopf bifurcation, complex conjugate eigenvalue pair is located at the imaginary axis and oscillations may arise or disappear at this point. The Jacobian matrix is non-singular at the Hopf bifurcation. Whereas in the case of limit-induced bifurcations, the lack of steady state solutions are due to system controls reaching limits (e.g. generator reactive power limits).

2.7 Examples of Voltage Instability

To analyze the voltage instability, a simple 2-bus power system network is chosen and is shown in Figure 2.4. The system consists of a load fed from a voltage source E through a

transmission line modeled as a series reactance. The load bus voltage can be written as

$$V \angle \delta = E - jX\bar{I} \quad (2.1)$$

The apparent power S transmitted over the line to the load is:

$$S = P + jQ = \bar{V}\bar{I}^* = V \angle \delta \frac{\bar{E}^* - \bar{V}^*}{-jX} \quad (2.2)$$

$$= \frac{j}{X} (EV \cos \delta + jEV \sin \delta - V^2) \quad (2.3)$$

The active and reactive power delivered to the load can be written as

$$P = -\frac{EV}{X} \sin \delta \quad (2.4)$$

$$Q = \frac{EV}{X} \cos \delta - \frac{V^2}{X} \quad (2.5)$$

From Equation 2.4 and 2.5, the value of the load bus voltage is given as

$$V^2 = \frac{E^2}{2} - QX \pm X \sqrt{\frac{E^4}{4X^2} - P^2 - Q \frac{E^2}{X}} \quad (2.6)$$

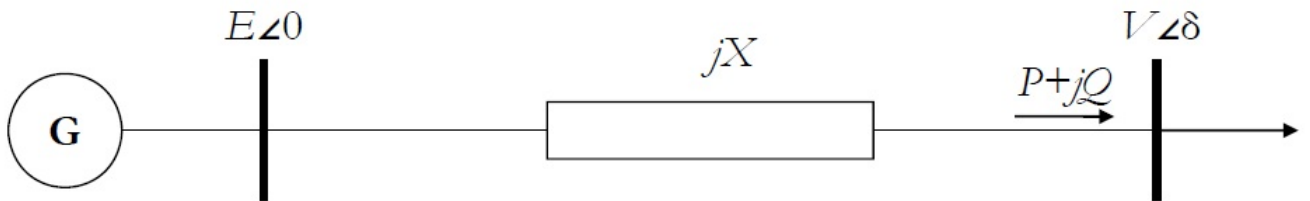


Figure 2.4: Single line diagram of a two bus system.

For various load values with different constant power factors, the variation of voltage with respect to real power is shown in Figure 2.5. From the Figure 2.5 it is observed that as power factor increases, voltage stability margin is increases.

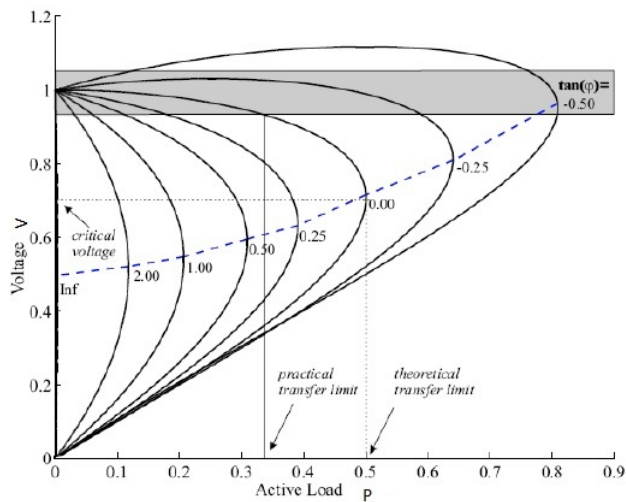


Figure 2.5: Variation of voltage with real power for different power factors.

Figure 2.6 shows that as the load on the system is increased, the system moves towards the voltage collapse point. Before reaching the voltage collapse point, there exist several equilibrium points of operation. After crossing the loadability limit, the system collapses as equilibrium is lost.

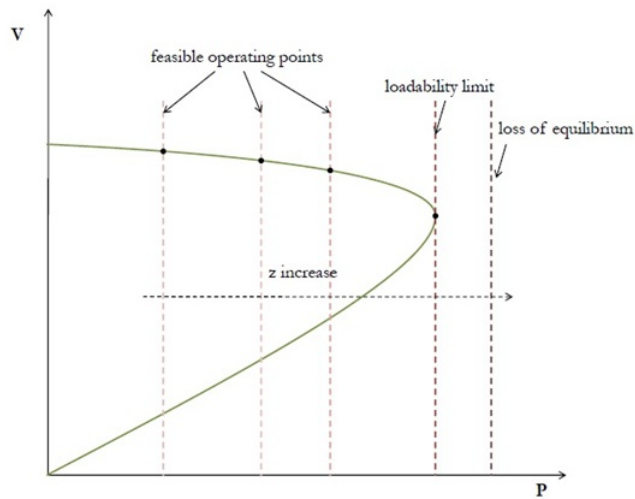


Figure 2.6: Loss of equilibrium with gradual increase in load.

When a disturbance occurs like removal of line, loss of generation or a fault occurs then the voltage stability margin decreases. If the system is continued to operate without

any control actions, system performance will be affected. Figure 2.7 shows the reduced voltage stability margin when a disturbance is occurred.

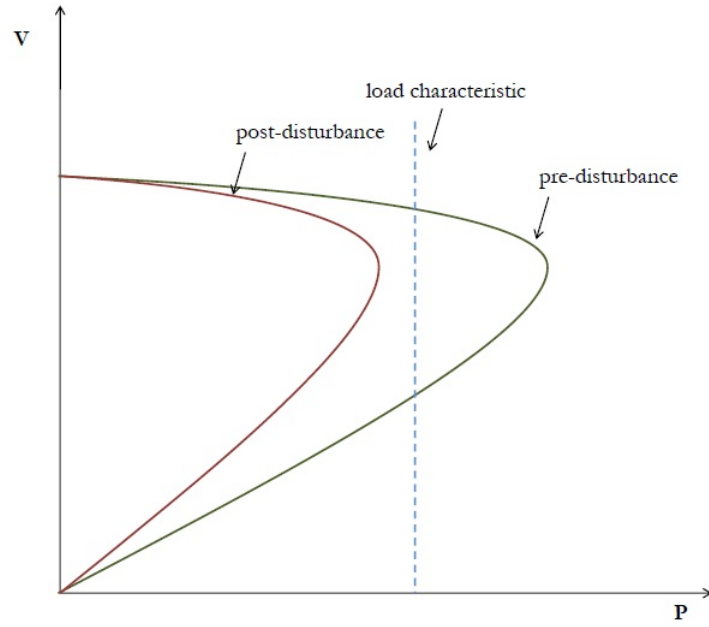


Figure 2.7: Reduced voltage stability margin following a disturbance.

Chapter 3

Load Modeling and Countermeasures for Voltage Collapse

3.1 Introduction to Load Modeling

The modeling of loads is essential in voltage stability analysis. The voltage dependence and dynamics of loads requires attention in the analysis. For accuracy, voltage dependent load models are represented at the secondary side of distribution system main transformer including possible tap changer control. The dynamics of loads in long-term voltage stability studies includes the operation of load tap changers, compensation, thermostatic loads, protection systems which operates due to low voltage. Load modeling is a difficult problem because power system loads are aggregates of many devices.

3.1.1 Static Load Modeling

A static load model [3] is a model where the power is a function of voltage and/or the frequency but without time dependency. Static loads are usually modeled with an exponential or polynomial model. The value of exponent describes the voltage dependence of the load. Integer values of exponents zero, one and two corresponds to constant power, constant current and constant impedance loads respectively. The exponent load model is presented in Equation 3.1 and 3.2.

$$P = P_0 \left(\frac{V}{V_0} \right)^\alpha \quad (3.1)$$

$$Q = Q_0 \left(\frac{V}{V_0} \right)^\beta \quad (3.2)$$

where P is active load, Q is reactive load. P_0 is base active load, Q_0 is base reactive load. V is load voltage, V_0 is base load voltage. α is exponent of active load, β is exponent of reactive load. The typical values for exponents of different load components are presented in Table 3.1.

Table 3.1: Typical values for exponents of load model [3]

load component	α	β
incandescent lamps	1.54	-
room air conditioner	0.50	2.5
furnace fan	0.08	1.6
battery charger	2.59	4.06
Fluorescent lighting	0.95-2.07	0.31-3.21

Generally loads are aggregates of many devices and polynomial load model (ZIP model) is used to represent the load and it is shown in Equation 3.3 and 3.4.

$$P = P_0 \left(Z_p \left(\frac{V}{V_0} \right)^2 + I_p \left(\frac{V}{V_0} \right) + P_p \right) \quad (3.3)$$

$$Q = Q_0 \left(Z_q \left(\frac{V}{V_0} \right)^2 + I_q \left(\frac{V}{V_0} \right) + Q_q \right) \quad (3.4)$$

The frequency dependency of load can be represented using the following load model.

$$P = P_0 \left(Z_p \left(\frac{V}{V_0} \right)^2 + I_p \left(\frac{V}{V_0} \right) + P_p \right) [1 + Z_{pf}(f - f_0)] \quad (3.5)$$

The parameters of polynomial load models are Z_p , I_p and P_p for active power and Z_q ,

I_q and Q_q for reactive power, which describes the share of components of total load and $Z_p+I_p+P_p=1$, $Z_q+I_q+Q_q=1$. The exponential load model has advantage of having only two parameters instead of four in the ZIP load model. This is an advantage for the identification of individual loads.

3.1.2 Dynamic Load Modeling

The dynamic load model presents a time dependency that generally describes a recovery of the load. Following a voltage dip, load reacts instantaneously before recovering towards a power closer to the previous load consumption. This class of model can describe phenomena as different as fast recovery of a motor or slow recovery of a thermostatic controlled load. one of the dynamic load model is a composite load model [3]. It is made of ZIP load model which represents static part of the load and an induction motor model which represents the dynamic part of the load.

Another dynamic load model is proposed by Hill and Karlsson [17] [18] to represent the thermostatic and load tap changer recovery of the load which occurs with long time constants in distribution feeders. This model is described by the following equations:

$$T_p \dot{P}_r + P_r = N_p(V) \quad (3.6)$$

$$P_d = P_r + P_i(V) \quad (3.7)$$

$$(3.8)$$

with

$$N_p(V) = P_s(V) - P_i(V) \quad (3.9)$$

$$P_i(V) = P_0 \left(\frac{V}{V_0} \right)^{\alpha_i} \quad (3.10)$$

$$P_s(V) = P_0 \left(\frac{V}{V_0} \right)^{\alpha_s} \quad (3.11)$$

where P_d is the final load consumption. The steady state P_s and instantaneous P_i load behavior are voltage dependent with an exponent α_s and α_i respectively. T_p is the recovery

time constant and P_0 is the steady state load consumption when the voltage V is equal to nominal voltage V_0 .

3.2 Countermeasures for Voltage Collapse

Countermeasures can be taken at various system design stages ranging from power system planning to real-time. The report [19] offers a complete classification of all the countermeasures that may be used to avoid voltage collapse. Few corrective actions are summarized here after:

- Load Tap Changer (LTC) control modification:

LTCs are an important cause of voltage instability because their action follows a load restoration [20]. Tap changers may be blocked on the current tap which prevents further deterioration of voltage magnitude. The set point used by LTC controller may be decreased. The LTC logic may be reversed [21] for restoring the voltage in the high voltage side instead of low voltage side. This can be done by decreasing load side voltage which also decrease load power.

- Load shedding:

Even though load shedding [22] is a disruptive practice, it is a very effective countermeasure against voltage collapse. In most cases, it results in an immediate voltage improvement. Several successive load shedding may be performed to get back to an acceptable voltage. This countermeasure is very cost effective. Its implementation is simple and the risk of occurrence of voltage instability is small. However, disturbance will be caused to consumers due to load shedding so this option should be consider as the very last of countermeasure.

- Action on generation devices:

- Generation devices includes generators and reactive compensation devices. The following actions [23] may be taken as countermeasures.
- Switching on capacitive compensation and switching off induction compensation are generally taken when loading level is very high.

- Increasing the voltage set point of generators will cause an increase in the voltage, decrease in current and thus a decrease in the loading of the transmission system. This action is effective only if the load behaves nearly as a constant power load. For the load to be a constant power load, the LTC should be active.
- Generation rescheduling and/or starting up of gas turbine or hydro-generation will help to meet the peak load. If small generation plants are available in the voltage stability affected areas, their starting up will greatly increase the stability. Generation rescheduling is a more complex action that must be optimized in simulations before it can be implemented.

Chapter 4

Methods of Voltage Stability

Analysis

4.1 Introduction

The analysis of voltage stability can be done using different methods. One of the mostly used method is finding the maximum loading point using the P-V curve or the Q-V curve with the help of power flow calculations. In this method, the distance between operating point and maximum loading point is taken as the stability criterion. Voltage stability analysis also can be done by using bifurcation as the stability criterion. Minimum singular value or minimum eigenvalue helps to find the critical operating point. Modal analysis in which system is represented by using eigenvectors is also used. At the voltage collapse point, solution of power flow equations experiences convergence problem. So to avoid this convergence problem, voltage stability indices are proposed based on power flow equations. These indices gives information such as critical buses and critical branches.

In this chapter, MATLAB simulation is performed on IEEE standard 6 bus and 14 bus system.

4.2 Real Power Margin Computation Using The P-V curve

In voltage stability analysis, relation between power transfer to the load and voltage of the load bus is not weak. Variation in power transfer from one bus to another bus effects the bus voltages. This can be studied using P-V curve.

For a network, load buses (PQ buses) are identified to plot the P-V curves. The load model is taken as constant real power which is represented by Equation 4.1.

$$P = P_0(1 + \lambda K_L) \quad (4.1)$$

Where P_0 is the base case load real power, λ is loading factor and K_L is the load increment factor. The power-flow solution of the system is taken as a base case.

Steps in P-V curve analysis:

1. Select a load bus, vary the load real power using loading factor λ and load increment factor K_L . Keep the power factor as constant.
2. Compute the power flow solution for the present load condition and record the voltage of the load bus.
3. Increase the loading factor by small amount and repeat step 2 until power flow does not have convergence.
4. P-V curve is plotted using the calculated load bus voltages for increased load values.
5. Real power margin is computed by subtracting the base load value from maximum load value at which voltage collapse occurs.

In P-V curve shown in Figure 4.1, there are three regions related to real power load P. In the first region up to loadability limit, power flow equation has two solutions for each P of which one is stable voltage and other is unstable voltage. If load is increased, two solutions will coalesce and P is maximum. If load is further increased, power flow equation

doesn't have a solution. Voltage corresponding to "maximum loading point" is called as critical voltage.

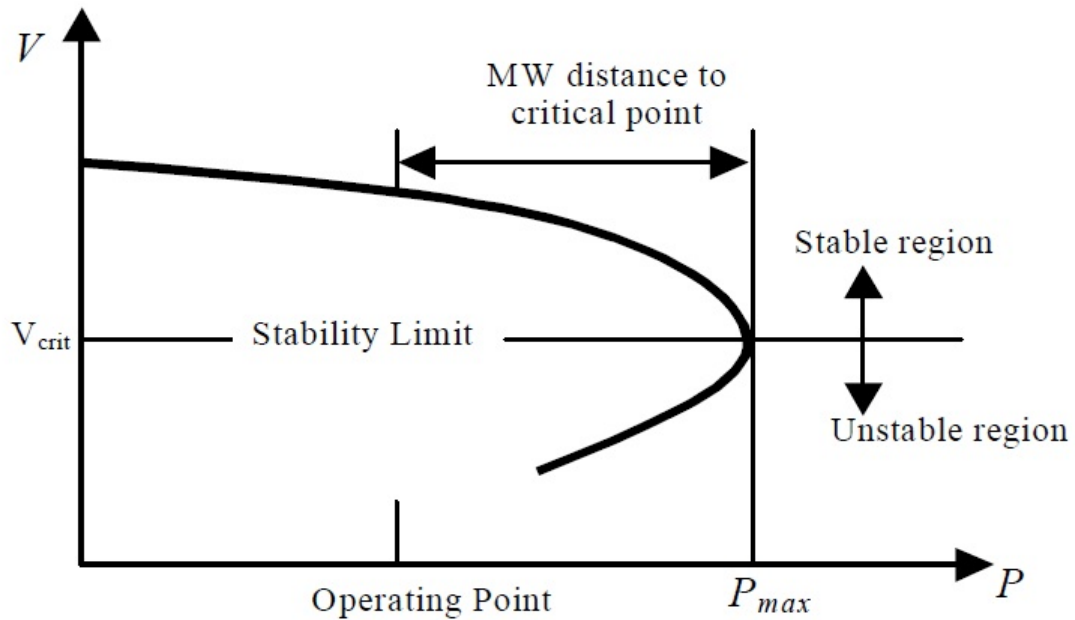


Figure 4.1: Typical P-V curve.

4.3 Reactive Power Margin Computation Using The Q-V curve

The V-Q curves, gives reactive power margin. It shows the reactive power injection or absorption for various scheduled voltages. If reactive power load is scheduled instead of voltages Q-V curves are produced. Q-V curves are a more general method of assessing voltage stability. Many utilities uses Q-V curves to determine the proximity to voltage collapse and to establish system design criteria based on Q and V margins. Q-V curves can be used to check whether the voltage stability of the system can be maintained or not and to take suitable control actions. A typical V-Q curve is shown in Figure 4.2

Near the collapse point of Q-V curve, sensitivities get very large and then reverse sign. Also, it can be seen that the curve shows two possible values of voltage for the

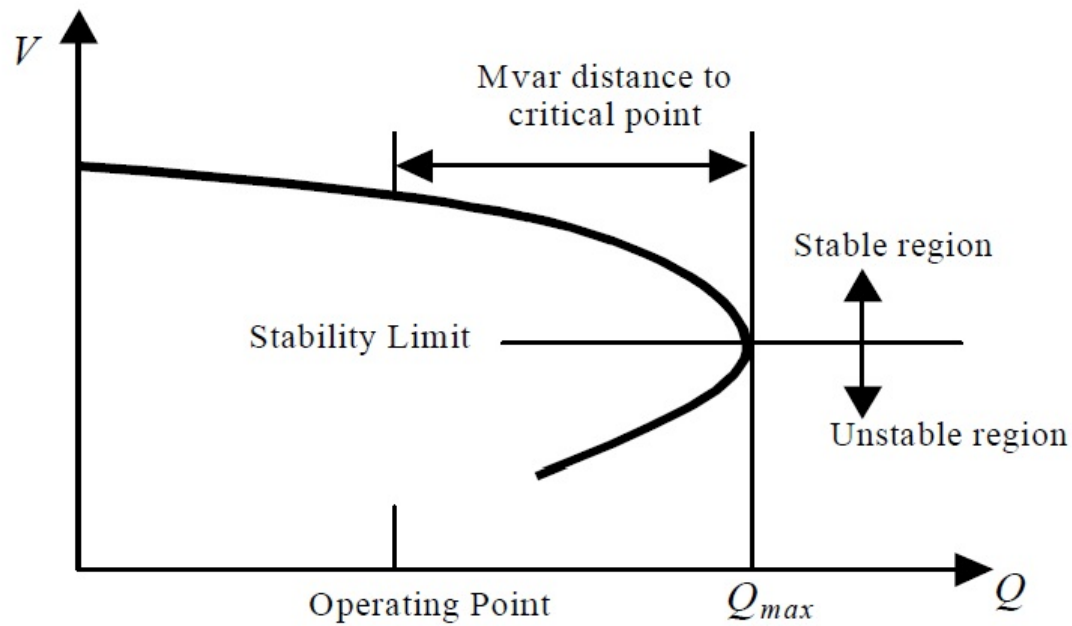


Figure 4.2: Typical Q-V curve.

same value of power. The power system operated at lower voltage value would require very high current to produce the power. That is why the bottom portion of the curve is classified as an unstable region and system can't be operated in this region.

Constant reactive power load model is selected and represented by the following Equation 4.2.

$$Q = Q_0(1 + \lambda K_L) \quad (4.2)$$

Where Q_0 is the base case load reactive power, λ is loading factor and K_L is the load increment factor. The power-flow solution of the system is taken as a base case.

Steps in Q-V curve analysis:

1. Select a load bus, vary the load reactive power using load demand factor λ and load increment factor K_L . Keep the real power of load as constant.
2. The reactive power output of each generator should be allowed to adjust.
3. Compute the power flow solution for the present load condition and record the voltage of the load bus.

4. Increase the load demand factor λ by small amount and repeat step 3 until power flow does not have convergence.
5. Q-V curve is plotted using the calculated load bus voltages for increased load values.
6. Reactive power margin is computed by subtracting the base load value from maximum load value at which voltage collapse occurs.

4.4 Disadvantages of P-V curves and Q-V curves

Though both methods are widely used as index to find the proximity to voltage collapse, but they have few disadvantages.

- In both methods, at a time only one bus is considered for load variation. As there is no information about critical buses, power flow studies are to be done for many buses which takes so much time.
- As the loading on the system approaches critical point, convergence problem occurs in solving the power flow equation.
- These methods doesn't give useful information about the causes of voltage instability.

4.5 Minimum Singular Value Method

Minimum singular value method is proposed as an index to find the proximity to voltage collapse point by Thomas and Lof [9]. This method is based on Jacobian matrix J_R of the power system. In this method, determinant of J_R is calculated until it reaches a minimum value by increasing the load on the system. This will give only proximity to voltage collapse but not provides specific causes of voltage instability such as critical lines and generators reaching reactive limits. As the system exhibits non linear behavior from stable operating point to bifurcation limit, it can't give a linear or absolute measure to voltage collapse point.

4.6 Continuation Power Flow Method

Continuation Power Flow (CPF) method overcomes problems like convergence problem near the voltage collapse point and computational time as in P-V and Q-V curves. Continuation power flow finds a next stable operating point for given load/generation change scenario. It can be used for tracing the whole P-V curve. The continuation load-flow finds the solution path of a set of load-flow equations that are reformulated to include a continuation parameter. The method is based on prediction-correction [10] technique. The intermediate results of the continuation process also provide valuable insight into the voltage stability of the system and the areas prone to voltage collapse. P-V curve solution using prediction-correction technique is shown in Figure. To apply continuation technique, the power flow equations must be reformulated to include a load parameter, λ . So the new power flow equations are expressed as a function of voltage V , angle of the buses δ and load parameter λ . Reformulated power flow equations at a bus i are

$$\Delta P_i = P_{Gi}(V, \delta, \lambda) - P_{Li}(V, \delta, \lambda) - P_{Inji} = 0 \quad (4.3)$$

$$\Delta Q_i = Q_{Gi}(V, \delta, \lambda) - Q_{Li}(V, \delta, \lambda) - Q_{Inji} = 0 \quad (4.4)$$

where

$$P_{Inji} = \sum_{j=1}^n V_i V_j y_{ij} \cos(\delta_i - \delta_j - \theta_{ij})$$

$$Q_{Inji} = \sum_{j=1}^n V_i V_j y_{ij} \sin(\delta_i - \delta_j - \theta_{ij})$$

and

$$0 \leq \lambda \leq \lambda_{cr}$$

P_{Inji} , Q_{Inji} are real and reactive power injection at bus i . P_{Gi} , Q_{Gi} are real and reactive power generation at bus i . P_{Li} , Q_{Li} are real and reactive power consumption at bus i .

$\lambda = 0$ corresponds to the base case and $\lambda = \lambda_{critical}$ to the critical case.

The voltage at bus i is $V_i \angle \delta_i$ and $y_{ij} \angle \theta_{ij}$ is the $(i, j)^{th}$ element of the system admittance

matrix Y_{BUS} .

For simulating different load change scenarios, loads are modified as

$$P_{Li}(\lambda) = P_{Li0}[1 + \lambda K_{Li}] \quad (4.5)$$

$$Q_{Li}(\lambda) = P_{Li0} \tan(\phi_i)[1 + \lambda K_{Li}] \quad (4.6)$$

where P_{Li0} , Q_{Li0} are the base real and reactive load at bus i . K_{Li} is multiplier designating the rate of load change at bus i as λ changes. ϕ_i is power factor of load at bus i .

The real power generation is modified to

$$P_{Gi}(\lambda) = P_{Gi0}[1 + \lambda K_{Gi}] \quad (4.7)$$

The steady state system is represented as

$$F(\delta, V, \lambda) = 0 \quad (4.8)$$

The prediction step estimates the next P-V curve solution based on a known solution.

Tangent vector is calculated from the following equation

$$[F_\delta, F_V, F_\lambda] \begin{bmatrix} d\delta \\ dV \\ d\lambda \end{bmatrix} = 0$$

where $T = [d\delta, dV, d\lambda]^T$ is the tangent vector and Jacobian matrix is augmented by one column with F_λ . Tangent vector can be determined as the solution of the equation

$$\begin{bmatrix} F_\delta & F_V & F_\lambda \\ & e_k & \end{bmatrix} [t] = \begin{bmatrix} 0 \\ \pm 1 \end{bmatrix} \quad (4.9)$$

where e_k is an appropriately dimensioned row vector with all elements equal to zero except

the k^{th} , which equal to one. If the index k is chosen properly, and $t_k = \pm 1$ guarantees that the augmented Jacobian matrix is non singular at the point of voltage collapse.

Once the tangent vector is calculated from Equation 4.9, the prediction of next operating point is calculated as

$$\begin{bmatrix} \delta^* \\ V^* \\ \lambda^* \end{bmatrix} = \begin{bmatrix} \delta \\ V \\ \lambda \end{bmatrix} + \sigma \begin{bmatrix} d\delta \\ dV \\ d\lambda \end{bmatrix} \quad (4.10)$$

where σ is a scalar designating step size. Next step is to correct the predicted solution. Local parameterization is used by which the set of original equations is augmented by one equation specifying the value of one of the state variables. It is expressed as

$$\begin{bmatrix} F(x) \\ x_k - \eta \end{bmatrix} = 0 \quad (4.11)$$

where η is an appropriated value for the k^{th} element of state variable x which consists (δ, V) .

4.6.1 Critical point identification

Continuation power flow is stopped when critical point is reached. Critical point is arrived at when loading on the system becomes maximum and then decreases. At critical point, the tangent vector component corresponding to loading factor λ is zero and becomes negative once it passes the critical point.

4.7 Modal Analysis

Modal analysis is carried mainly depending on the power-flow Jacobian matrix J . The matrix J is reduced to J_R by keeping real power as constant. The mismatch power

vector can be written as Equation

$$\begin{bmatrix} \Delta P \\ \Delta Q \end{bmatrix} = [J] \begin{bmatrix} \Delta \delta \\ \Delta V \end{bmatrix} \quad (4.12)$$

where

$$J = \begin{bmatrix} J_{P\delta} & J_{PV} \\ J_{Q\delta} & J_{QV} \end{bmatrix} \quad (4.13)$$

By substituting $\Delta P = 0$ in above Equation 4.12:

$$\begin{aligned} \Delta P = 0 &= [J_{P\delta}\Delta\delta + J_{PV}\Delta V] , \\ \Delta\delta &= -J_{P\delta}^{-1}J_{PV}\Delta V \end{aligned}$$

and

$$\Delta Q = J_R\Delta V \quad (4.14)$$

where

$$J_R = [J_{QV} - J_{Q\delta}J_{P\delta}^{-1}J_{PV}] \quad (4.15)$$

The reduced Jacobian matrix J_R represents the linearized relationship between the incremental changes in bus voltage (ΔV) and bus reactive power injection (ΔQ).

The reduced Jacobian matrix J_R is represented with it's eigenvector matrices and shown in Equation 4.16

$$J_R = \xi \Lambda \eta \quad (4.16)$$

where ξ =right eigenvector matrix of J_R

η =left eigenvector matrix of J_R

Λ =diagonal eigenvalue matrix of J_R

Reduced Jacobian matrix J_R can be written as

$$J_R^{-1} = \xi \wedge^{-1} \eta \quad (4.17)$$

$$\text{where} \quad \xi \eta = I \quad (4.18)$$

Equation 4.14 can be written as

$$\Delta V = \xi \wedge^{-1} \eta \Delta Q \quad (4.19)$$

$$\text{or} \quad (4.20)$$

$$\Delta V = \sum_i \frac{\xi_i \eta_i}{\lambda_i} \Delta Q \quad (4.21)$$

where

λ_i is the i^{th} eigenvalue, ξ_i is the i^{th} column right eigenvector and η_i is the i^{th} row left eigenvector of matrix J_R . Each eigenvalue defines one mode of the system operation. The i^{th} modal reactive power variation is defined as:

$$\Delta Q_{mi} = K_i \xi_i \quad (4.22)$$

where K_i is a normalization factor so that

$$K_i^2 \sum_j \xi_{ji}^2 = 1 \quad (4.23)$$

where ξ_{ji}^2 is the j^{th} element of ξ_i . The corresponding i^{th} modal voltage variation is:

$$\Delta V_{mi} = \frac{1}{\lambda_i} \Delta Q_{mi} \quad (4.24)$$

As the system is stressed, the value of λ_i becomes smaller and modal voltage becomes weaker. If magnitude of $\lambda_i = 0$, the corresponding modal voltage collapses since it undergoes infinite changes for reactive power changes. System is defined as voltage stable if all the eigenvalues of J_R are positive. Voltage collapse point is reached when at least one of the eigenvalue reaches zero. If any of eigenvalues are negative, the system is unstable.

4.7.1 Identification of critical buses and branches

Once the voltage collapse point is reached, left and right eigenvectors are calculated corresponding to critical mode. The bus participation factor for measuring the participation of the k^{th} bus in i^{th} mode is defined as

$$P_{ki} = \xi_{ki}\eta_{ki} \quad (4.25)$$

Bus participation factor corresponding to critical modes can predict areas or nodes in power system susceptible to voltage instability. Buses with large participation factors to the critical mode correspond to the most critical buses.

By knowing the values ΔV and $\Delta\delta$, the linearized reactive power loss (ΔQ_{lji}) variation across all transmission branch lj are calculated. Branch participation factor of branch lj to mode i can be calculated as

$$P_{lji} = \frac{\Delta Q_{lji}}{\max(\Delta Q_{lji})} \quad (4.26)$$

Branches with large participation factors to critical mode are identified as critical branches. These branches consumes the most reactive power flowing in the network.

4.8 Voltage Stability Indices

The condition of voltage stability in a power system can be characterized by the use of voltage stability index. This index can either referred to a bus or a line. Voltage stability indices are derived from the basic power flow equation. Voltage stability indices are helpful in determining the proximity of a given operating point to voltage collapse point. These indices are simple, easy to implement and computationally inexpensive. Voltage stability indices can be used for both on-line or off-line studies.

4.8.1 Fast Voltage Stability Index (FVSI)

I. Musirin [13] derived a voltage stability index based on a power transmission concept in a single line

The 2-bus power system model is shown in Figure 4.3 and this is used to derive FVSI. In the 2- bus power system model,

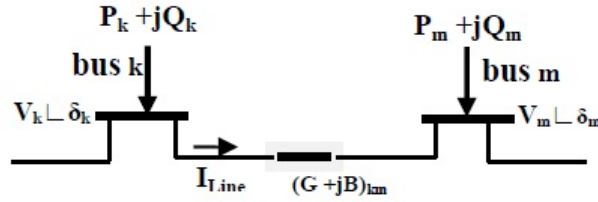


Figure 4.3: 2-bus power system model.

V_k, V_m are the sending and receiving end voltages

P_k, P_m are the sending and receiving end real power

Q_k, Q_m are the sending and receiving end reactive power

δ_k, δ_m are the sending and receiving end bus voltage angles

The current through the line is given by

$$I_{Line} = \frac{V_k \angle \delta_k - V_m \angle \delta_m}{R + jX} \quad (4.27)$$

The apparent power at bus m is given as

$$S_m = V_m \angle \delta_m I_{Line}^* \quad (4.28)$$

Rearranging the Equation 4.28 gives

$$I_{Line} = \left(\frac{S_m}{V_m \angle \delta_m} \right)^* \quad (4.29)$$

$$I_{Line} = \frac{P_m - jQ_m}{V_m \angle -\delta_m} \quad (4.30)$$

From Equation 4.27 and 4.30,

$$\frac{V_k \angle \delta_k - V_m \angle \delta_m}{R + jX} = \frac{P_m - jQ_m}{V_m \angle -\delta_m} \quad (4.31)$$

$$V_k \angle \delta_k V_m \angle -\delta_m - V_m^2 = (R + jX)(P_m - jQ_m) \quad (4.32)$$

separating the real and imaginary parts gives

$$V_k V_m \cos(\delta_k - \delta_m) - V_m^2 = RP_m + XQ_m \quad (4.33)$$

and,

$$-V_k V_m \sin(\delta_k - \delta_m) = XP_m - RQ_m \quad (4.34)$$

Substituting P_m from the Equation 4.34 into Equation 4.33 gives a quadratic equation of V_m ;

$$V_m^2 - \left(\frac{R}{X} \sin(\delta) + \cos(\delta) \right) V_k V_m + \left(X + \frac{R^2}{X} \right) Q_m = 0 \quad (4.35)$$

where $\delta = \delta_k - \delta_m$

The condition to obtain real roots for V_m is

$$\frac{4Q_m X Z^2}{V_k^2 (R \sin(\delta) + X \cos(\delta))} \leq 1 \quad (4.36)$$

Since δ is normally very small then, $\delta \approx 0$, $R \sin(\delta) \approx 0$ and $X \cos(\delta) \approx X$

The Fast Voltage Stability Index(FVSI) for a line k-m is

$$FVSI_{km} = \frac{4Z^2 Q_m}{V_k^2 X} \quad (4.37)$$

When the FVSI of a line approaches unity it means that the line is approaching its stability limits. The FVSI of all the lines must be lower than 1 to assure the stability of power system.

4.8.2 Line stability index L_{mn}

Moghavvemmi [14] derived a voltage stability index based on a power transmission concept in a single line. In Figure 4.3, a 2-bus power system model is shown. The reactive power injected at bus m is given as

$$Q_m = \frac{V_k V_m}{Z} \sin(\theta_{km} - \delta_k + \delta_m) - \frac{V_m^2}{Z} \sin \theta \quad (4.38)$$

Where θ_{km} is angle of $(k, m)^{th}$ element of system admittance matrix Y_{bus} . Putting $\delta_k - \delta_m = \delta$ in the Equation 4.38 and it is solved for V_m . Then the value of V_m is

$$V_m = \frac{V_k \sin(\theta - \delta) \pm \sqrt{[V_k \sin(\theta - \delta)]^2 - 4ZQ_m \sin \theta}}{2 \sin \theta} \quad (4.39)$$

To get real roots of V_m , the discriminant should be greater than zero so the line stability index is given as

$$L_{mn} = \frac{4Q_m X}{[V_k \sin(\theta - \delta)]^2} \quad (4.40)$$

When L_{mn} values of a line approaches unity it means that the line is approaching its stability limits. The L_{mn} values of all the lines must be lower than 1 to assure the stability of power system.

4.8.3 Voltage reactive power index VQI

Voltage reactive power index VQI is simple and accurate in voltage stability analysis. Computational time is less. This index can be used for on-line applications. M.W. Mustafa et.al. [15] proposed voltage reactive power index as

$$VQI_{Line} = \frac{4Q_m}{|Y_{km}| \sin(\theta_{km}) V_k^2} \quad (4.41)$$

This index determines voltage stability at each line and predicts system voltage collapse. Once the value of VQI_{Line} approaches unity, the voltage stability reaches stability limits. VQI_{Line} determines how far the power system is from collapse point.

4.8.4 Voltage stability index L

Voltage stability index L is used for monitor the voltages of the buses. P.Kessel derived L index [16] based on load flow results. L index is given as

$$L_j = \left| 1 - \sum_{i=1}^{i=g} \bar{F}_{ji} \frac{\bar{V}_i}{\bar{V}_j} \right| \quad (4.42)$$

Where g= no of generators

\bar{V}_i is the i^{th} bus voltage

\bar{V}_j is the j^{th} bus voltage

\bar{F}_{ji} is the element of F matrix

F matrix is obtained as below

$$\begin{bmatrix} \bar{I}^G \\ \bar{I}^L \end{bmatrix} = \begin{bmatrix} \bar{Y}^{GG} & \bar{Y}^{GL} \\ \bar{Y}^{LG} & \bar{Y}^{LL} \end{bmatrix} \begin{bmatrix} \bar{V}^G \\ \bar{V}^L \end{bmatrix} \quad (4.43)$$

where \bar{I}^G, \bar{I}^L and \bar{V}^G, \bar{V}^L represent currents and voltages at the generator buses and load buses. The matrix \bar{F}^{LG} is calculated as

$$\bar{F}^{LG} = -[\bar{Y}^{LL}]^{-1}[\bar{Y}^{LG}] \quad (4.44)$$

The L-indices are calculated for all load buses. L-index calculation is simple and results are consistent.

4.9 Simulation Results and Discussions

4.9.1 Introduction

Voltage stability analysis is carried out for determining loadability limits for IEEE standard 6-bus and 14-bus power systems. Newton-Raphson method is used for solving the power flow equations. MATLAB code is written for the used methods.

4.9.2 Results for IEEE standard 6-Bus system

The IEEE standard 6-Bus system consists of two synchronous generators and three loads. Real power margin is calculated from P-V curve. P-V curves are drawn for constant power and constant current load models for all load buses. P-V curve results for constant power load model are shown in the Table 4.1 and Figure 4.4.

Table 4.1: Real power margin of load buses for constant power load model of IEEE 6-bus system

Bus No	Critical loading factor λ_{cr}	Real power margin (P_{margin} in p.u)	Critical voltage (V_{cr} in p.u)
3	0.9310	3.2258	0.6340
5	0.8120	0.6340	0.5362
6	0.9080	2.2632	0.6083

The P-V curves are plotted in Figure 4.4. From the Table 4.1 and Figure 4.4, it is observed

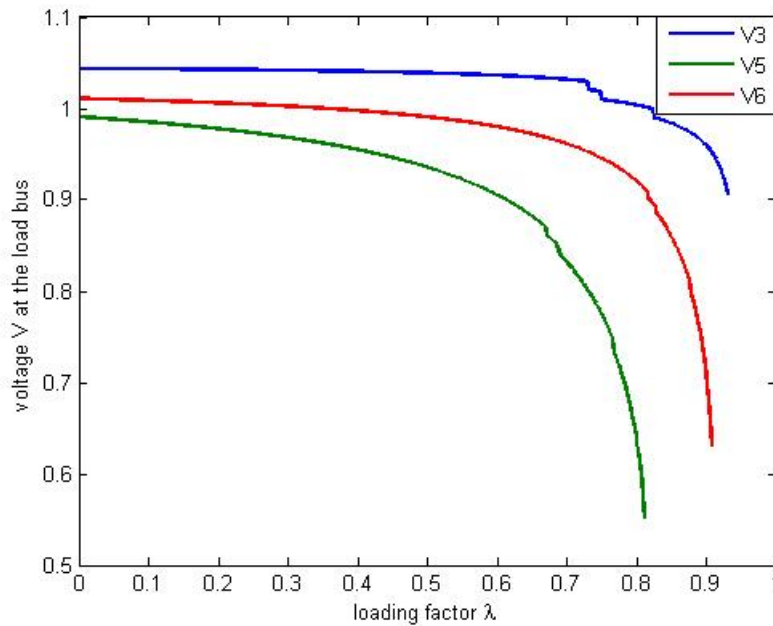


Figure 4.4: The P-V curves of load buses for constant power load of IEEE 6-bus power system.

that bus number 5 is having least real power margin when constant power load model is

used in the analysis.

The P-V curve results for constant current load model are shown in the Table 4.2 and Figure 4.5.

Table 4.2: Real power margin of load buses for constant current load model of IEEE 6-bus system

Bus No	Critical loading factor λ_{cr}	Real power margin (P_{margin} in p.u)	Critical voltage (V_{cr} in p.u)
3	1.09	3.7056	0.9093
5	1.67	1.3036	0.5373
6	1.65	0.5373	0.5782

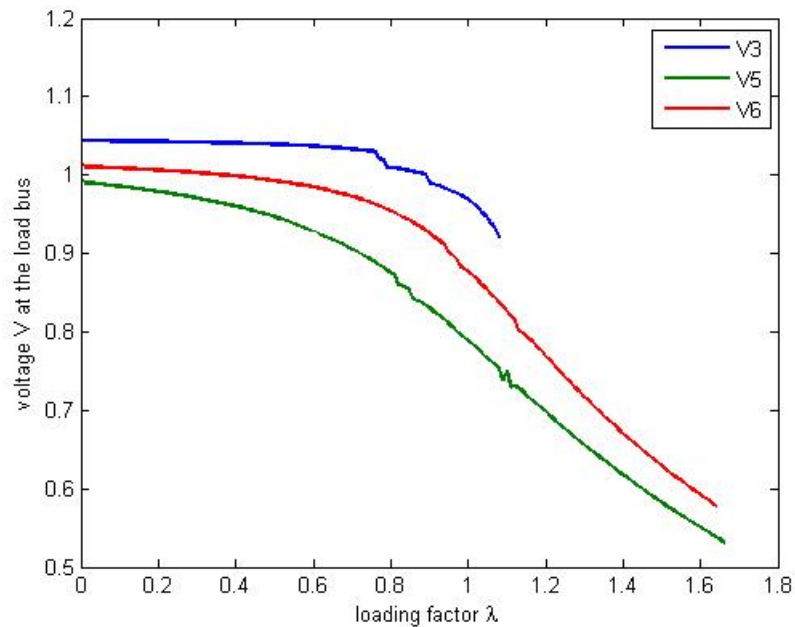


Figure 4.5: The P-V curves of load buses for constant current load of IEEE 6-bus power system.

From the above results, it is observed that real power margin of bus 6 is small and it is the critical bus.

The Q-V curves for constant power load model are shown in Figure 4.6. Reactive power margin of load buses are given in Table 4.3. Results of the Q-V curves shows that bus 5 is having least reactive power margin and it is the critical bus.

Table 4.3: Reactive power margin of load buses of IEEE 6-bus system

Bus number	3	5	6
Reactive power margin(in p.u)	2.7244	1.3973	1.7978

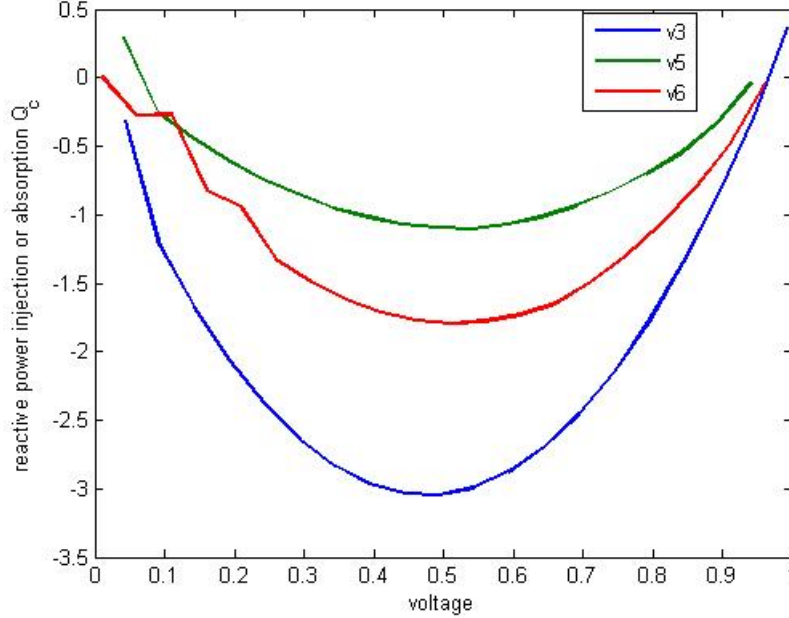


Figure 4.6: The Q-V curves of load buses of IEEE 6-bus power system.

Continuation power flow method is applied to calculate the real power loading margin. It gives a operating point and voltages with respect to loading factor λ are shown in Figure 4.7. Voltage curve of bus 5 is showing sharp decrease in the slope and its voltages reaching low values at the critical point. The critical loading factor $\lambda_{critical} = 0.85$, is obtained using Continuation power flow method. Where as in P-V curves, the obtained least loading factor is $\lambda_{critical} = 0.812$ which is for bus 5. These two values are nearer to each other. Bus 5 is identified as a critical bus.

Modal analysis is performed by varying only load reactive power. The minimum eigenvalues of J_R represents critical modes of operation. Corresponding to this mode of operation bus participation and branch participation factors are calculated. Variation of minimum eigenvalue with loading is shown in Figure 4.8. The bus participation factors of load buses are shown in Figure 4.9. It is observed that bus 5 is having largest participation factor

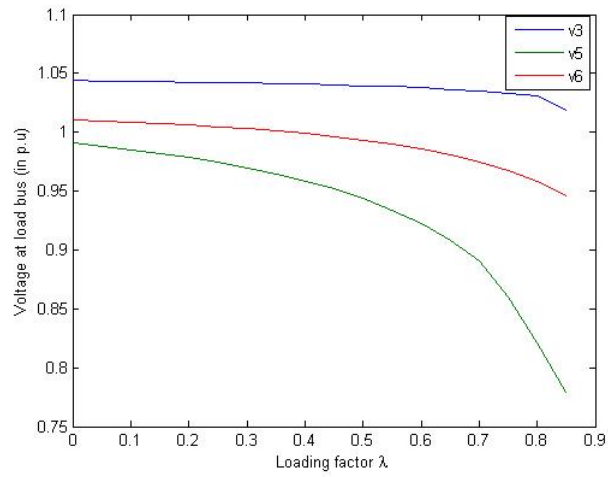


Figure 4.7: Critical loading factor using Continuation power flow method.

and it is sensitive to voltage instability. The Branch participation factors of branches are shown in Figure 4.10. Branch 4 has largest participation factor and it is consuming most of the reactive power that is available in the network.

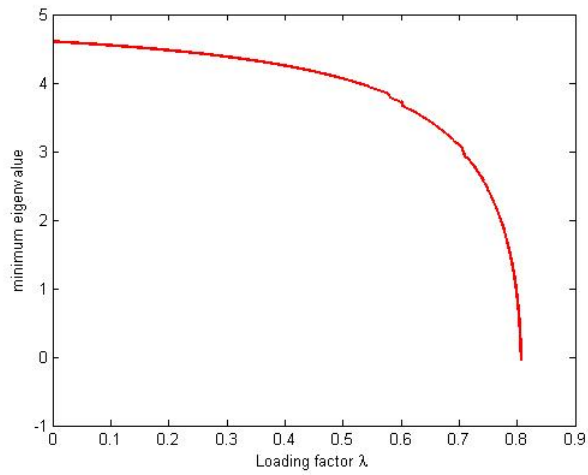


Figure 4.8: Path of minimum eigenvalue with increase of loading.

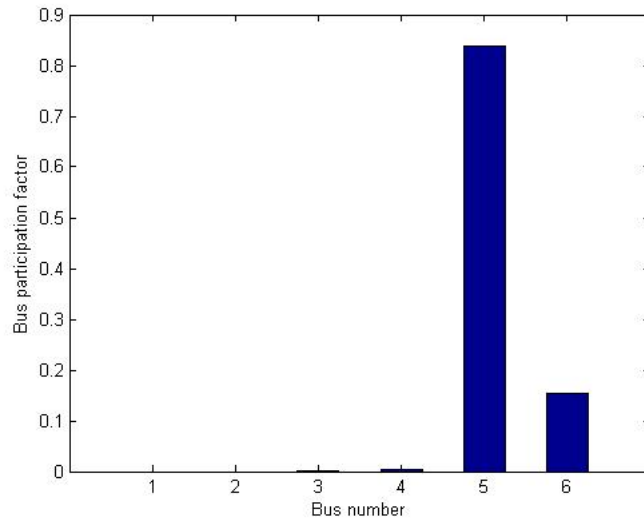


Figure 4.9: Bus Participation factors for most critical modes for the IEEE 6-bus system.

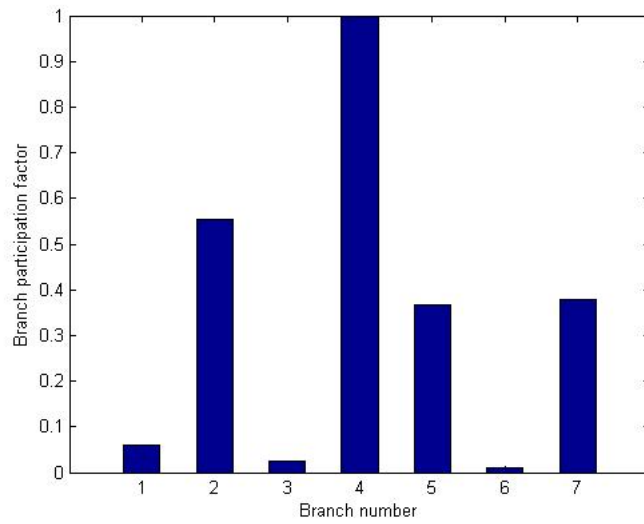


Figure 4.10: Branch Participation factors for most critical modes for the IEEE 6-bus system.

4.9.3 Results for IEEE Standard 14-bus System

The IEEE 14-bus standard system is considered for the analysis and it consists five generators and three synchronous condensers.

By considering constant power load model, the P-V curves are drawn for all load buses in Figure 4.11. The real power margin of all the load buses are plotted in Figure 4.12.

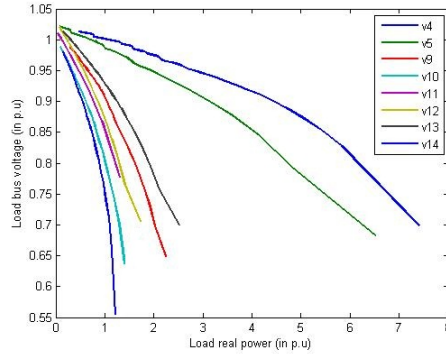


Figure 4.11: The P-V curves of IEEE 14 bus system for constant load model.

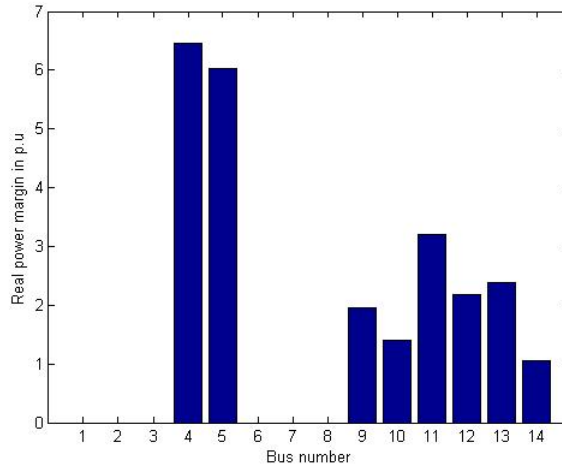


Figure 4.12: Real power margin for constant power load model of IEEE 14-bus system.

From the Figures 4.11 and 4.12, it is observed that bus 14, 10 and 9 are having least real power margin in decreasing order respectively.

The load model is changed to constant current load model and the P-V curves are plotted in Figure 4.13.

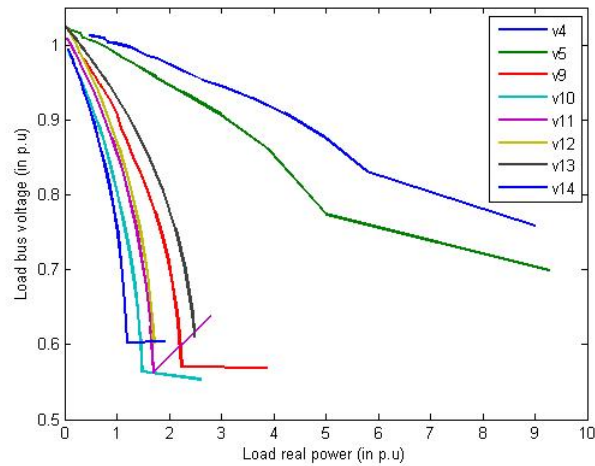


Figure 4.13: The P-V curves for constant current load model of IEEE 14-bus system.

The real power margin of load buses for constant current load model are shown in Figure 4.14.

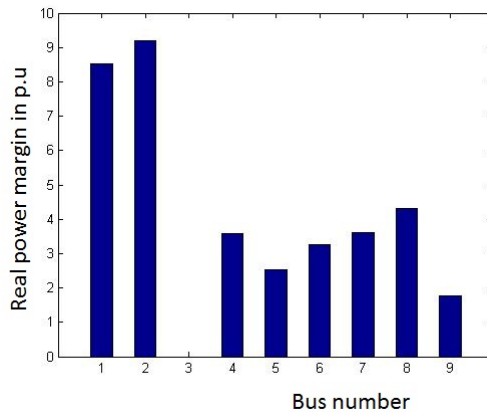


Figure 4.14: Real power margin for constant current load model of IEEE 14-bus system.

When the load model is changed to constant current model, real power margins are increased and this is due to voltage dependency of the load model.

The system is simulated by removing a line from bus 9 to 14, which decreases the real power margin of bus 14. It is shown in Figure 4.15.

Continuation power flow method is applied for finding real power margin for the critical buses 14, 10 and 9. The real power margin calculated from continuation power flow

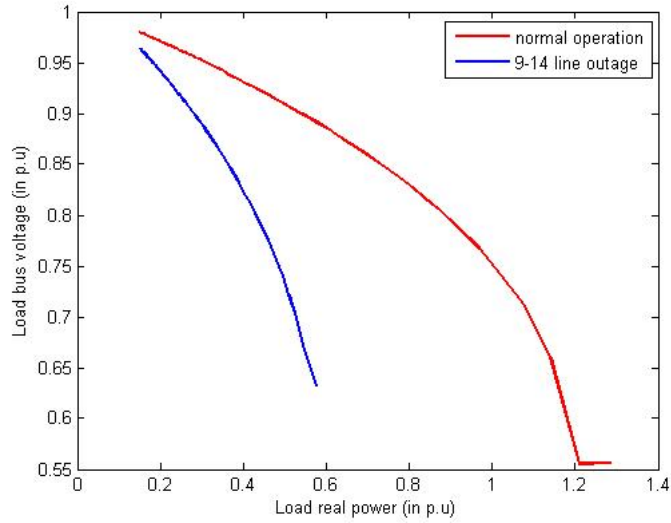


Figure 4.15: Reduced Real power margin of Bus 14 following the outage of line 9-14.

method and P-V curves are shown in Table 4.4

Table 4.4: Comparison of Real power margin of Critical buses 14, 10 and 9 using P-V curves and CPF method

Bus number	Real power margin using P-V curve (in p.u)	Real power margin using CPF method (in p.u)
14	1.0635	1.0098
10	1.2674	1.2258
9	1.9496	1.9993

The Q-V curves are plotted in Figure 4.16. These curves are plotted by scheduling voltages at the load buses. The value of reactive power in the plot is the required amount of reactive power to be injected or consumed at the load bus to maintain the scheduled voltage.

Figure 4.17 shows that the reactive power margin of all the load buses of IEEE 14-bus system. From the Figure 4.17, it is observed that bus 14, 10 and 9 are very sensitive buses because they have limited amount of reactive power margin.

Modal analysis is performed for IEEE 14-bus system. Minimum eigenvalue indicates critical mode of operation and the path of minimum eigenvalue is shown in Figure 4.18. Bus and branch participation factors are shown in the Figures 4.19 and 4.20. It is observed

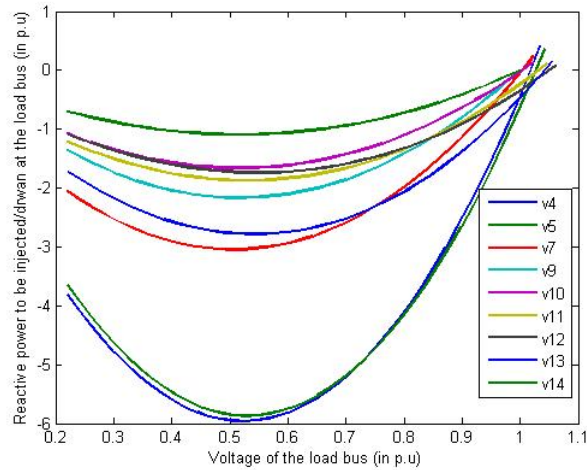


Figure 4.16: The Q-V curves for constant power load model of IEEE 14-bus system.

that bus 14, 10 and 9 are showing voltage instability. From Figure 4.20, it is observed that branches 15, 20 and 11 are heavily loaded and are close to collapse limits.

Voltage stability indices are calculated for single load increase and multiple load increasing scenarios. Load at bus 14 is increased and the indices are calculated. Fast Voltage Stability Index (FVSI) and line stability index (LMN) are almost equal whereas Voltage reactive power index (VQI) is closer to both. The variation of FVSI, LMN and VQI indices for critical branch 20 with respect to loading factor λ is shown in Figure 4.21. As the loading approaches critical point, these indices slowly increase and move towards one. Bus 14, 10 and 9 are the critical buses. The voltage of the critical bus 14 is shown in Figure 4.22. All the voltage stability indices are calculated for increase in loads at all load buses and the behavior of the indices for critical branch 20 is shown in Figure 4.23. Branches 15, 11 and 20 are the critical branches.

The behavior of line stability index and voltage of the bus 14 is shown in Figure 4.24.

All the voltage stability analysis methods are revealing that bus 14, 10 and 9 are the critical buses and they least reactive power margin in descending order.

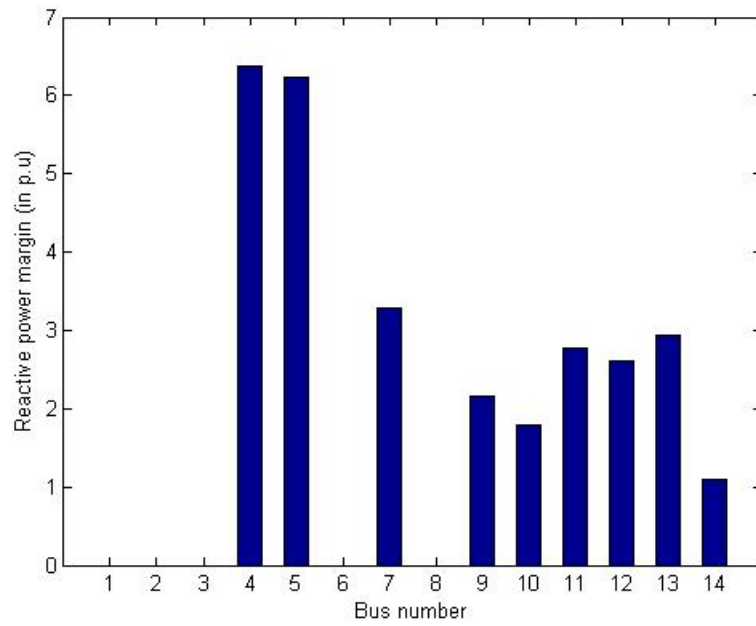


Figure 4.17: Reactive power margin for constant power load model of IEEE 14-bus system.

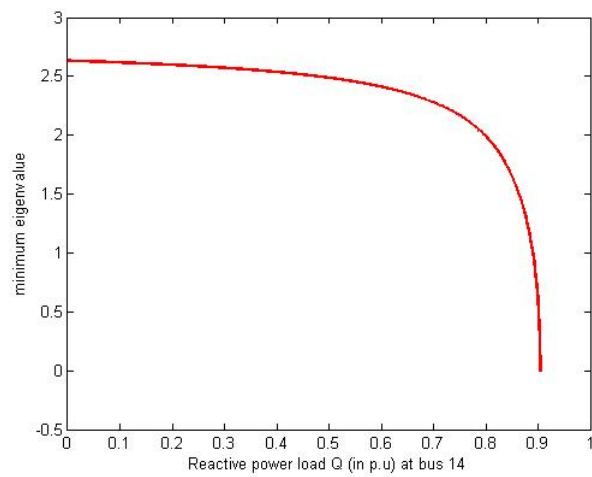


Figure 4.18: Path of minimum eigenvalue with increase of load for IEEE 14-bus system.

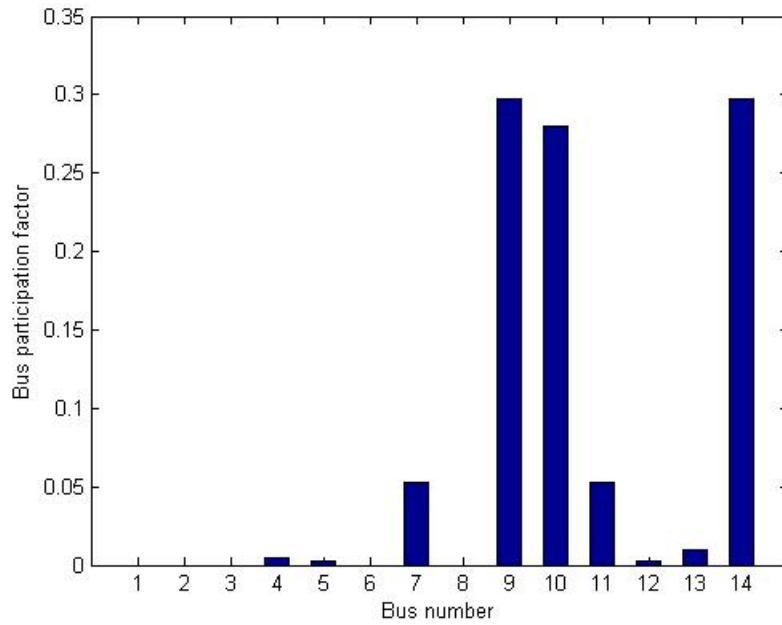


Figure 4.19: Bus participation factors for IEEE 14-bus system.

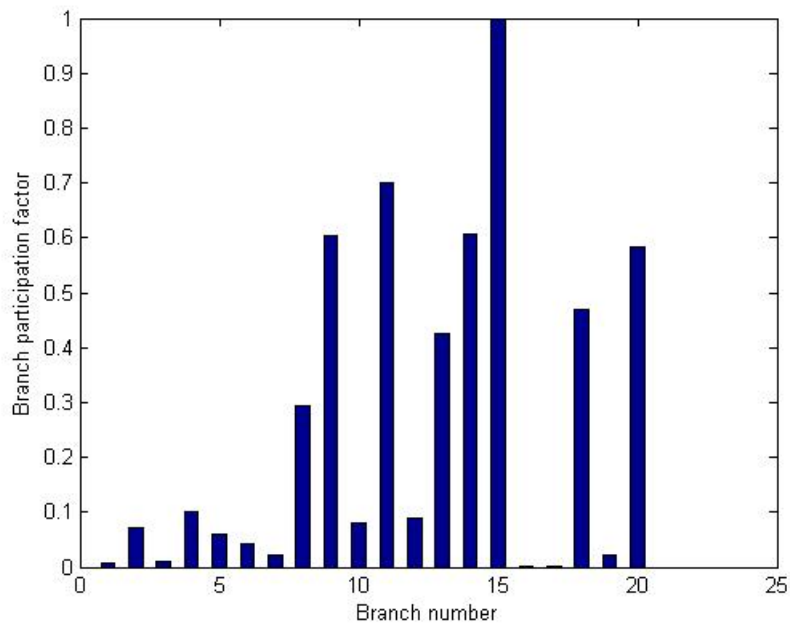


Figure 4.20: Branch participation factors for IEEE 14-bus system.

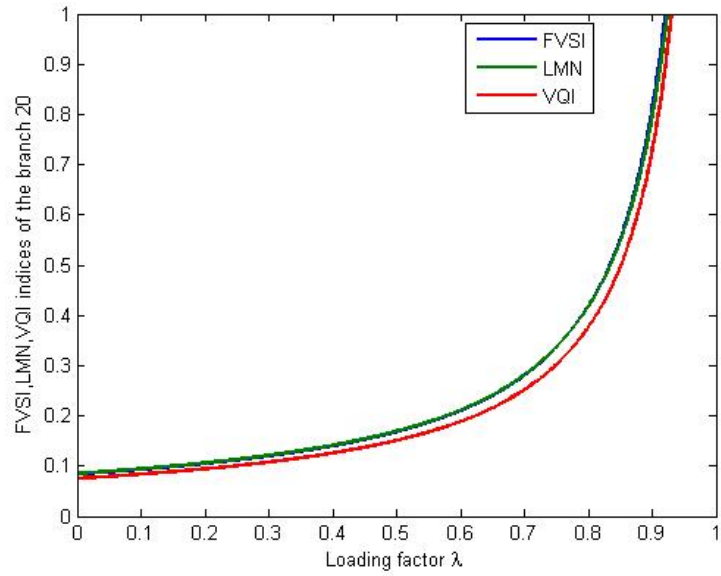


Figure 4.21: The variation of voltage stability indices FVSI, LMN and VQI for critical branch with loading factor λ .

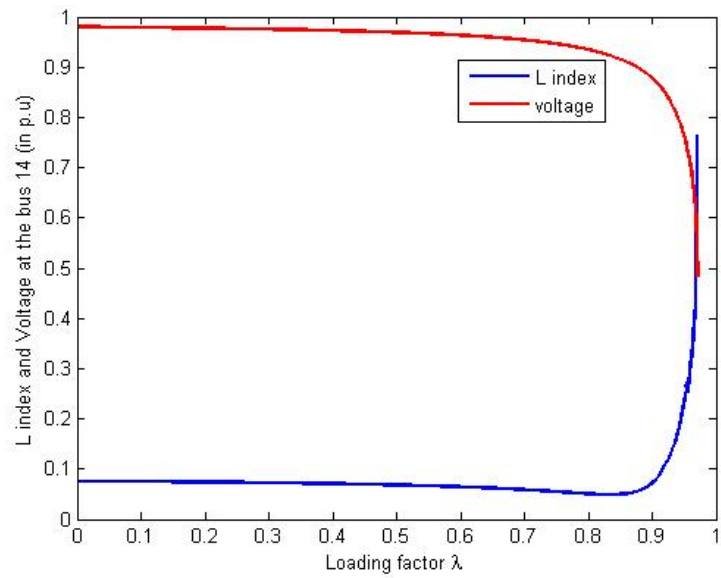


Figure 4.22: The variation of line stability index L, voltage of bus 14 with loading factor λ .

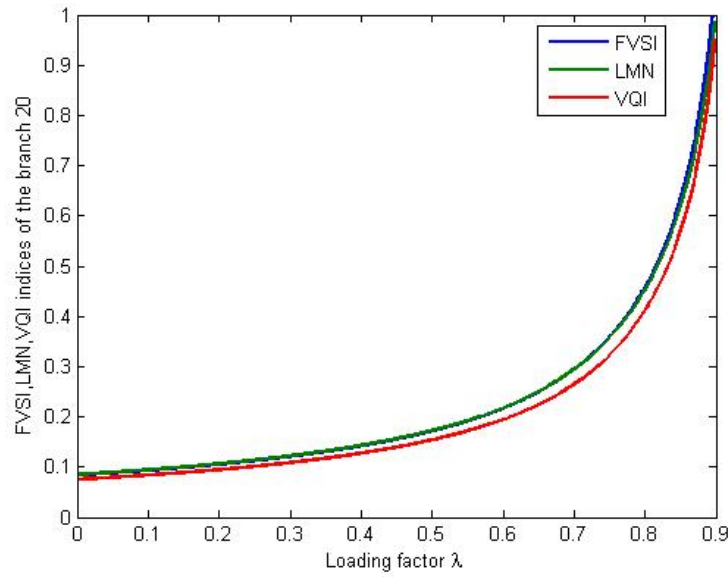


Figure 4.23: The variation of voltage stability indices FVSI, LMN and VQI with loading factor λ for multiple load increase scenario.

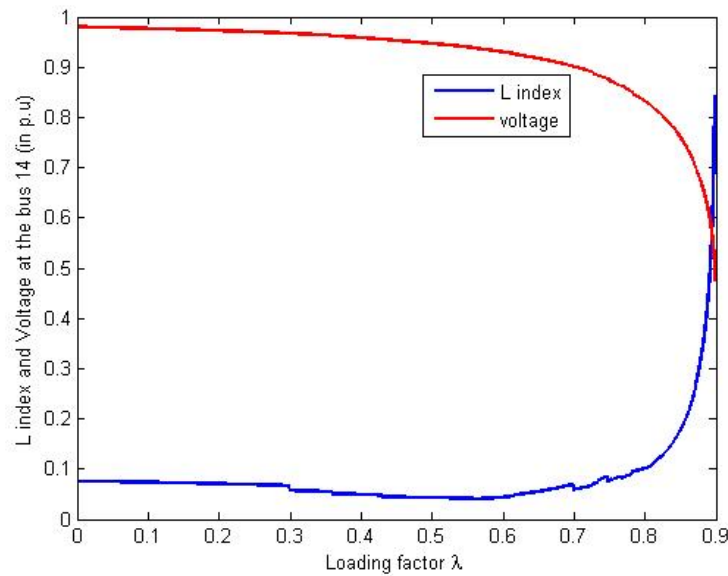


Figure 4.24: The variation of line stability index L, voltage of bus 14 with loading factor λ for multiple load increase scenario.

Chapter 5

Conclusions and Future Scope of Research

5.1 Conclusions

In this work, voltage stability problem is analyzed in view of maximum loadability limit. Simulations are carried out on IEEE standard 6 bus and 14 bus systems. Load modeling is an important aspect in voltage stability analysis and various load models are therefore considered.

P-V curves and Q-V curves are drawn for various load buses with different load models. From these curves, maximum loadability limit is computed.

The maximum loadability limit is calculated using continuation power flow method in which the power-flow solutions are traced. Critical loading factor is calculated and it is nearly equal to that of from P-V curves.

Modal analysis is used and the maximum loadability is identified at the smallest minimum eigenvalue of the reduced system Jacobian matrix J_R . This method gives bus participation factors and branch participation factors that are used to identify the critical buses and critical branches.

To crosscheck the modal analysis results, Q-V curves are drawn for critical buses and results are matched. These results are helpful for determining the amount of reactive power compensation. Critical buses are provided with reactive power compensation for

improving the voltage stability.

Voltage stability indices are calculated and voltage instability is observed for various loading scenarios. When the system is voltage stable, these indices are close to zero and move towards to 1 as system is gradually moving towards critical point. Different voltage stability indices are calculated and compared for single and multiple load change scenarios. Using these indices, Critical buses and branches are identified and these results are matching with that of Modal analysis.

5.2 Future Scope of Research

This work is useful for static voltage stability analysis. Future work can be done on dynamic voltage stability analysis by considering generator dynamics and dynamic load models. Dynamic analysis can be done for contingencies and ranking can be given for buses and branches. The improvement in voltage stability by various reactive power compensation devices can be observed.

Bibliography

- [1] P. Kundur, J. Paserba, V. Ajjarapu, G. Andersson, A. Bose, C. Canizares, N. Hatziargyriou, D. Hill, A. Stankovic, C. Taylor, T. Van Cutsem, and V. Vittal, “Definition and classification of power system stability,” *IEEE Transactions on Power Systems*, vol. 19, no. 2, pp. 1387-1401, May 2004.
- [2] C. D. Vournas, P. W. Sauer, and M. A. Pai, “Relationships between voltage and angle Stability of power systems,” *Electric Power Systems Research*, vol. 18, no. 8, pp. 493-500, November 1996.
- [3] T. Van Cutsem and C. Vournas, *Voltage Stability of Electrical Power Systems*. New York: Springer Science, 1998.
- [4] B. Gao, G. K. Morison, and P. Kundur, “Voltage stability analysis using Static and dynamic approaches,” *IEEE Transactions on Power Systems*, vol. 8, no. 3, pp. 1159-1171, Aug. 1993.
- [5] Luis Aromataris, Patricia Arnera, and Jean Riubrugent, “Improving static techniques for the analysis of voltage stability,” *Electric Power System Research*, vol. 33, no. 4, pp. 901-908, May 2011.
- [6] P. Kundur, *Power System Stability and Control*. New York: McGraw-Hill, 1994.
- [7] C.W. Taylor, *Power System Voltage Stability*. New York: McGraw-Hill, 1994.
- [8] C.A. Canizares, “Voltage stability assessment: Concepts, practices and tools,” *IEEE-PES Power Systems Stability Subcommittee Special Publication SP101PSS (ISBN 01780378695)*, 2003.

- [9] P.A. Lof, G. Anderson, and D.J.Hill, "Voltage stability indices for stressed power systems," *IEEE Transactions on Power Systems*, vol. 8, no. 1, pp. 326-335, Feb. 1993.
- [10] V. Ajjarapu and C. Christy, "The continuation power flow: A tool for steady state voltage stability analysis," *IEEE Transactions on Power Systems*, vol. 7, no. 1, pp. 416-423, Feb. 1992.
- [11] V. Ajjarapu, *Computational Techniques for Voltage Stability Assessment and Control*. New York: Springer Science, 2006.
- [12] B. Gao, G. K. Morison, and P. Kundur, "Voltage stability evaluation using modal analysis," *IEEE Transactions on Power Systems*, vol. 7, no. 4, pp. 1529-1542, Nov. 1992.
- [13] I. Musirin and T. K. Abdul Rahman, "Estimating maximum loadability for weak bus identification using FVSI," *IEEE Power Engineering Review*, pp. 50-52, Nov. 2002.
- [14] M. Moghavemmi and F.M. Omar, "Technique for contingency monitoring and voltage collapse prediction," *IEE Proceedings on Generation, Transmission and Distribution*, vol. 145, pp. 634-640, Nov. 1998.
- [15] F.A. Althowibi and M.W. Mustafa, "Voltage stability calculations in power transmission lines: Indication and allocations," *IEEE International Conference on Power and Energy*, pp. 390-395, Nov. 2010.
- [16] P. Kessel and H. Glavitsch, "Estimating the voltage stability of a power system," *IEEE Transaction on Power delivery*, vol. 1, no. 3, pp. 346-354, Jul. 1986.
- [17] D. Karlsson and D.J. Hill, "Modelling and identification of nonlinear dynamic loads in power systems," *IEEE Transactions on Power Systems*, vol. 9, no. 1, pp. 157-166, Feb. 1994.
- [18] D.J. Hill, "Nonlinear dynamic load models with recovery for voltage stability studies," *IEEE Transactions on Power Systems*, vol. 8, no. 1, pp. 166-176, Feb. 1993.

- [19] C. Henville (chair), “Voltage Collapse Mitigation,” *IEEE Power System Relaying Committee Working Group K12*, December 1996.
- [20] T.X. Zhu and S.K. Tso, “An Investigation into the OLTC effects on voltage collapse,” *IEEE Transactions on Power Systems*, vol. 15, no. 2, pp. 515-521, May 2011.
- [21] C.D. Vournas and M. Karystianos, “Load tap changers in emergency and preventive voltage stability control,” *IEEE Transactions on Power Systems*, vol. 19, no. 1, pp. 492-498, Feb. 2004.
- [22] Xu Fu and Xifan Wang, “Determination of load shedding to provide voltage stability,” *Electric Power System Research*, vol. 33, no. 3, pp. 515-521, March 2011.
- [23] T. Van Cutsem and C.D. Vournas, “Emergency voltage stability controls: an Overview,” *Proceedings of IEEE/PES General Meeting*, June 24-28, 2007.